JOURNAL OF GEOPHYSICAL RESEARCH, VOL. 107, NO. D20, 10.1029/2000JD000309, 2002

A macroscale hydrological data set of river flow routing parameters for the Amazon Basin

Marcos Heil Costa, Carlos Henrique C. Oliveira, Ricardo G. Andrade,
Thiago R. Bustamante, and Fabrício A. Silva
Department of Agricultural Engineering, Federal University of Viçosa, Viçosa, Minas Gerais, Brazil

Michael T. Coe
Center for Sustainability and the Global Environment (SAGE), Institute for Environmental Studies,
University of Wisconsin-Madison, Madison, Wisconsin, USA

Received 27 December 2000; revised 14 August 2001; accepted 14 August 2001; published 22 August 2002.

[1] Continental-scale hydrologic routing models, also known as macrohydrological routing models, have evolved considerably in the past few years. As the models have become more sophisticated, they have represented a variety of new processes and expanded their data requirements—either as input data or as validation for the model output. This paper presents a new data set of large-scale hydrological river flow routing parameters for the Amazon and Tocantins basins. Part of this data set was required by the development of the continental-scale hydrological routing model HYDRA and its application to the Amazon Basin. HYDRA represents phenomenalike floods, backwater effects, and seasonal hydrograph much more realistically than the previous generation of macrohydrological routing models. The data set contains data on (1) river network at 5-min (~9 km) resolution, (2) time series of monthly means of river discharge and river stage for 122 fluviometric stations spread throughout the basin, (3) sinuosity of each of the main rivers measured at 111 river sections in the basin, and (4) depth to the water table and transmissivity of the aquifer derived from measurements taken at 81 points throughout the basin. *INDEX TERMS:* 1833 Hydrology: Hydroclimatology; 1860 Hydrology: Runoff and streamflow; 3322 Meteorology and Atmospheric Dynamics: Land/atmosphere interactions; 9360 Information Related to Geographic Region: South America; *KEYWORDS:* Amazonia, macroscale hydrology, river network, river sinuosity

1. Introduction

[2] The Amazon Basin is the largest watershed in the world, with an area of 6.7 M km^2 (including the Tocantins river basin). The Amazon is also the largest river of the world in discharge, alone contributing about 20% of all the fresh water transported to the oceans. The discharge of the Amazon River is five times as large as the discharge of the world's second largest river, the Zaire. Even the tributaries of the Amazon would be among the top ten rivers of the world, if they were considered separately.

[3] The Large-Scale Biosphere-Atmosphere Experiment in Amazonia (LBA) examines how changes in land cover and climate can affect the functioning of the Amazonian ecosystem. One of the science questions that LBA proposed to answer is "what would be the response in the volume and timing of flow in the River Amazon to the changes in climate (...), or which may occur as a result of large-scale change in land use?" This type of question typically will be answered with the help of climate models coupled to large-scale hydrological routing models.

[4] Large-scale hydrologic routing models, also known as macrohydrological routing models, have evolved considerably in the past several years. Initial river transport models using the cell-to-cell routing methodology [e.g., *Vörösmarty et al.*, 1989; *Miller and Russell*, 1992; *Liston et al.*, 1994; *Miller et al.*, 1994; *Marengo et al.*, 1994; *Sausen et al.*, 1994; *Costa and Foley*, 1997; *Hagemann and Dümenil*, 1998] were usually based on the conservation of mass, using an empirical linear reservoir function to transfer the water through the groundwater and channel reservoirs.

[5] New model formulations, however, may represent a process by a more sophisticated methodology or, furthermore, may represent a variety of new processes. For example, *Stieglitz et al.* [1997] presented an approach where the fundamental hydrologic unit is the watershed rather than the soil column. *Arora and Boer* [1999] use formulations for the river flow velocity that includes the geometry of the channel and simulates the stage of the river.

[6] Another example is HYDRA by *Coe* [2000]. The Hydrological Routing Algorithm simulates the time-varying flow and storage of water in terrestrial hydrological systems, including rivers, floodplains, wetlands, lakes, and human-made reservoirs. Rivers, lakes, wetlands, and floodplains are defined as a continuous hydrologic network in which locally derived runoff accumulates and is transported across the land surface in rivers, fills lakes and wetlands, overflows riverbanks and is eventually transported to the ocean or is evaporated from an inland water body. This

0148-0227/02/2000JD000309$09.00

Figure 1. The basin.

model currently operates on the global scale at 5-min by 5-min latitude/longitude (~9 km at the equator) spatial resolution.

[7] The development of such models is closely associated to the availability of the required input data, as well as data for validation of the model output. HYDRA, for example, requires input data like the geometry of the riverbank and validation data can include river stage (from fluviometric stations or remote sensing) and flood extension (usually from remote sensing).

[8] In addition, the Amazon Basin hydrological system is unique. The Amazon region is mainly a very flat region, with an extensive potentially flooded area, where topographic gradients are very small, if existent at all. In this case, bidirectional exchanges of water between the flooded part of the river and the groundwater reservoir can be important. A methodology to model the bidirectional exchanges is under development and testing, requiring data on aquifer transmissivity. Finally, an accurate estimate of the total volume of water stored in the river channel requires a better knowledge of the length of the river, along with channel and riverbank geometrical characteristics.

[9] This paper presents a new data set of continental-scale hydrological river flow routing parameters for the Amazon and Tocantins basins (Figure 1). The data set contains data on (1) river network, at 5 min (~9 km) resolution, (2) time series of monthly means of river discharge and river stage, for 122 fluviometric stations spread throughout the basin, (3) sinuosity of each of the main rivers, measured at 111 river sections in the basin, and (4) depth of the water table and transmissivity of the aquifer, derived from measurements taken at 81 points throughout the basin. The specific data sets are described in the remainder of the paper.

2. River Network and Basin Border

[10] Although there are several global river network data sets available [*Graham et al.*, 1999; *Renssen and Knoop*, 2000; *Vörösmarty et al.*, 2000], and some of them have good error control techniques, they present several routing inconsistencies that are usually acceptable in a global data set, but become much more evident in regional simulations.

[11] In this section, we describe a data set of the river network of the Amazon and Tocantins river basin. The data are presented in gridded format at the resolution of 5 min of arc (~9 km). Four sources are used to assemble and validate the data set: (1) a 1:1,000,000 map of Northern South America, (2) a 1:5,000,000 hydrogeological map of South America, (3) the global river network digital data set by *Graham et al.* [1999], and (4) a data set of drainage areas upstream of specific points (fluviometric stations), provided by ANEEL (the Brazilian Agency for Waters and Electrical Energy).

[12] The construction of this part of the data set required three steps: (1) determination of the basin borders, (2) determination of the river network, and (3) refinement of the river network to assure quality sinuosity data. Each of these steps is described briefly below. The final river network at 5-min resolution is presented in Figure 2.

2.1. Determination of the Basin Borders

[13] Initially, two borders were drawn independently. The first one was digitized from a 1:5,000,000 hydrogeological map of South America, which has the borders of the Amazon and Tocantins basins marked. The second one was digitized from a 1:1,000,000 map of Northern South America [*Brazil-IBGE*, 1972]. This map does not show the basin borders, so it is assumed that the border would be in the middle point between nearby rivers that run into and out of the basin. Then, the two maps were overlaid and an initial version of the basin mask was obtained by careful analysis of the regions where the two borders disagreed. The final version was obtained together with the river network, to match the drainage areas of fluviometric stations, provided by ANEEL (see next step).

2.2. Determination of the River Network

[14] We started from the global river network data set by *Graham et al.* [1999], which had only the directions of the largest Amazon Basin rivers (e.g., the Amazon main stem, the Negro, the Madeira, etc.) properly geolocated, and the rest of the river network derived from a Digital Elevation Model. This data set was cropped using the initial version of

Figure 2. River network. In this figure, the darker the graytone, the higher the drainage area upstream.

Table 1. Fluviometric Stations and Errors in the Area Estimates

Number	River	Latitude	Longitude	Drainage area (km^2)		Error (%)
				ANEEL	Data set	
1	Javari at Estirão do Repouso	4°22′S	70°56′W	58,434	58,107	−0.6
2	Solimões at Teresina	4°17′S	69°44′W	969,497	983,157	1.4
3	Solimões at São Paulo de Olivença	3°28′S	68°45′W	980,717	990,781	1.0
4	Içа at Ipiranga Velho	2°59′S	69°35′W	108,006	108,362	0.3
5	Solimões at Santo Antônio do Içá	3°5′S	67°56′W	1,121,079	1,134,540	1.2
6	Juruá at Cruzeiro do Sul	7°37′S	72°40′W	38,504	38,537	0.1
7	Tarauacá at Envira	7°26′S	70°3′W	49,805	48,317	−3.0
8	Juruá at Gavião	4°50′S	66°45′W	162,174	162,000	−0.1
9	Japurá at Acanauí	1°48′S	66°33′W	238,390	242,259	1.6
10	Solimões at Itapeuá	4°3′S	63°1′W	1,753,684	1,769,000	0.9
11	Purus at Seringal Providência	8°55′S	68°36′W	37,280	37,636	1.0
12	Purus at Seringal da Caridade	9°2′S	68°34′W	62,894	63,166	0.4
13	Acre at Floriano Peixoto	9°3′S	67°23′W	33,270	33,468	0.6
14	Purus at Seringal Fortaleza	7°41′S	66°56′W	151,464	153,016	1.0
15	Ituxi at São Gregório	7°33′S	64°57′W	34,754	35,302	1.6
16	Purus at Labréa	7°15′S	64°48′W	218,270	220,351	1.0
17	Purus at Arumã-Jusante	4°41′S	62°7′W	353,741	359,853	1.7
18	Solimões at Manacapuru	3°19′S	60°35′W	2,187,719	2,147,730	−1.8
19	Uaupés at Taraquá	0°12′N	68°32′W	45,139	44,732	−0.9
20	Negro at Curicuriari	0°13′S	66°49′W	195,215	194,462	−0.4
21	Negro at Serrinha	0°27′S	64°50′W	281,639	279,945	−0.6
22	Branco at Caracaraí	1°48′N	61°8′W	125,089	124,980	−0.1
23	Guaporé at Pedras Negras	12°50′S	62°56′W	112,172	116,731	4.1
24	Mamoré at Guajará-Mirim	10°48′S	65°23′W	578,880	589,500	1.8
25	Madeira at Abunã	9°42′S	65°21′W	887,078	899,761	1.4
26	Abunã at Morada Nova	9°50′S	65°34′W	30,651	30,807	0.5
27	Madeira at Porto Velho	8°46′S	63°55′W	949,022	954,285	0.6
28	Ji-Paraná at Ji-Paraná	10°53′S	61°57′W	32,590	32,806	0.7
29	Ji-Paraná at Tabajara	8°55′S	62°6′W	61,744	60,212	−2.5
30	Madeira at Humaitá	7°30′S	63°1′W	1,063,101	1,066,240	0.3
31	Madeira at Manicoré	5°49′S	61°18′W	1,122,933	1,123,670	0.1
32	Aripuanã at Prainha	7°15′S	60°24′W	118,174	108,578	−8.1
33	Amazonas at Óbidos	1°54′S	55°30′W	4,623,731	4,618,746	−0.1
34	Arinos at Porto dos Gaúchos	11°39′S	57°14′W	34,773	36,207	4.1
35	Teles Pires at Cachoeirão	11°45′S	55°46′W	33,661	34,180	1.5
36	Teles Pires at Indeco	10°8′S	55°31′W	51,773	51,277	−1.0
37	São Manoel at Três Marias	7°38′S	57°53′W	141,472	137,485	−2.8
38	Tapajós at Barra São Manoel	7°19′S	58°5′W	332,386	332,163	−0.1
39	Tapajós at Jatobá	5°9′S	56°50′W	390,177	387,378	−0.7
40	Xingu at São Felix do Xingu	6°35′S	52°3′W	258,339	250,626	−3.0
41	Xingu at Belo Horizonte	5°23′S	52°53′W	283,260	277,265	−2.1
42	Curuá at Mouth	5°43′S	54°26′W	35,909	34,693	−3.4
43	Ririí at Pedra do Ó	4°34′S	54°3′W	126,209	123,827	−1.9
44	Xingu at Altamira	3°12′S	52°13′W	449,764	446,203	−0.8
45	Tocantins at São Felix (A/B)	13°32′S	48°8′W	55,580	57,062	2.7
46	Paranã at Ponte Paranã	13°15′S	47°15′W	30,787	29,818	−3.1
47	Fresco at Boa Esperança	6°43′S	51°46′W	42,589	42,275	−0.7
48	Paranã at Paranã	12°33′S	47°51′W	58,924	58,013	−1.5
49	Tocantins at Peixe	12°01′S	48°33′W	126,304	130,352	3.2
50	Tocantins at Porto Nacional	10°42′S	48°26′W	172,564	173,828	0.7
51	Tocantins at Miracema	9°33′S	48°24′W	183,968	186,834	1.6
52	Sono at Porto Real	9°11′S	48°02′W	45,620	44,910	−1.6
53	Tocantins at Tupiratins	8°14′S	48°06′W	242,902	243,841	0.4
54	Tocantins at Carolina	7°20′S	47°28′W	272,483	276,520	1.5
55	Tocantins at Tocantinópolis	6°19′S	47°25′W	287,993	290,570	0.9
56	Tocantins at Tucuruí	3°45′S	49°41′W	765,618	758,000	−1.0
57	Curuca at Santa Maria	4°41′S	71°28′W	24,416	24,351	−0.3
58	Ituí at Seringal do Ituí	4°44′S	70°18′W	19,126	19,103	−0.1
59	Juruá at Eirunepe-Montante	6°41′S	69°55′W	76,293	77,136	1.1
60	Acre at Xapuri	10°39′S	68°39′W	11,632	11,765	1.1
61	Acre at Rio Branco	9°58′S	67°48′W	22,947	22,670	−1.2
62	Purus at Valparaíso	8°42′S	67°24′W	102,604	103,285	0.7
63	Mucuim at Cristo	7°15′S	64°14′W	7308	7261	−0.6
64	Cuniua at Bacaba	6°20′S	64°55′W	38,349	38,270	−0.2
65	Negro at São Felipe	0°22′N	67°19′W	111,106	110,862	−0.2
66	Uaupés at Uaracu	0°33′N	69°10′W	40,847	40,506	−0.8
67	Uraricoera at Mocidade	3°27′N	60°57′W	44,976	44,483	−1.1
68	Uraricoera at Faz. Pássaro	3°14′N	60°39′W	51,742	50,985	−1.5
69	Mucajaí at Fé e Esperança	2°46′N	61°16′W	13,718	13,658	−0.4
70	Guaporé at Mato Grosso	15°01′S	59°58′W	17,851	18,412	3.1
71	Madeira at Palmeiral	9°32′S	64°49′W	924,159	936,801	1.4

Table 1. (continued)

Number	River	Latitude	Longitude	Drainage area (km^2)		Error (%)
				ANEEL	Data set	
72	Jamari at Ariquemes	9°56′S	63°04′W	7593	7295	−3.9
73	Jamari at São Carlos	9°42′S	63°08′W	10,214	9,884	−3.2
74	Jamari at São Pedro	8°59′S	63°17′W	13,007	12,733	−2.1
75	Jamari at Cachoeira do Samuel	8°45′S	63°28′W	14,448	14,135	−2.2
76	Candeias at Santa Isabel	8°48′S	63°43′W	12,177	12,728	4.5
77	Pimenta Bueno at Cachoeira Primavera	11°54′S	61°14′W	9388	9705	3.4
78	Pimenta Bueno at Pimenta Bueno	11°39′S	61°12′W	9724	10,114	4.0
79	Aripuana at Boca do Guariba	7°41′S	60°18′W	47,695	47,773	0.2
80	Sucunduri at Santarém Sucunduri	6°45′S	58°57′W	14,202	13,938	−1.9
81	Araguaia at Xambioá	6°23′S	48°33′W	368,644	364,496	−1.1
82	Curua at Boca do Inferno	1°34′S	54°50′W	20,341	20,803	2.3
83	Teles Pires at Porto Roncador	13°35′S	55°19′W	9398	9514	1.2
84	Teles Pires at Teles Pires	12°55′S	55°55′W	12,321	12,659	2.7
85	Verde at Lucas	13°09′S	55°57′W	5337	5327	−0.2
86	Curua-Una at Barragem-Jusante	12°47′S	54°16′W	18,158	17,982	−1.0
87	Maicuru at Arapari	1°45′S	54°25′W	17,250	17,072	−1.0
88	Paru de Este at Fazenda Paquira	0°25′S	53°43′W	30,463	30,945	1.6
89	Iriri at Laranjeiras	5°41′S	54°14′W	65,082	65,187	0.2
90	Jari at São Francisco	0°41′S	52°34′W	51,574	51,343	−0.4
91	Maranhão at Ponte Quebra Linha	14°59′S	48°43′W	11,177	11,008	−1.5
92	Almas at Ceres	15°16′S	49°35′W	10,162	10,538	3.7
93	Almas at Colônia dos Americanos	14°30′S	49°09′W	18,370	18,282	−0.5
94	Maranhão at Porto Uruacu	14°30′S	49°00′W	33,199	34,146	2.9
95	Paranã at Flores de Goiás	14°34′S	47°03′W	7213	7277	0.9
96	Paranã at Nova Roma	13°49′S	46°54′W	22,021	22,834	3.7
97	Paranã at Montante Barra do Palma	12°37′S	47°54′W	41,317	40,466	−2.1
98	Palma at Rio da Palma	12°24′S	47°10′W	12,494	12,527	0.3
99	Palma at Barra do Palma	12°33′S	47°49′W	17,523	17,547	0.1
100	Tocantins at Fazenda Angical	12°17′S	48°18′W	124,124	125,436	1.1
101	Santa Tereza at Colonha	12°19′S	48°40′W	8942	8690	−2.8
102	Santa Tereza at Jacinto	11°58′S	48°41′W	14,133	13,811	−2.3
103	Manuel Alves at Porto Jerônimo	11°44′S	47°52′W	10,674	10,373	−2.8
104	Manuel Alves at Fazenda Lobeira	11°31′S	48°19′W	14,457	14,462	0.0
105	Sono at Jatobá	10°06′S	47°18′W	14,101	13,855	−1.7
106	Sono at Novo Acordo	10°02′S	47°49′W	19,338	18,511	−4.3
107	Balsas at Porto Gilândia	10°44′S	47°48′W	8004	7735	−3.4
108	Balsas at Rio das Balsas	10°00′S	48°00′W	12,224	11,862	−3.0
109	Perdida at Dois Irmãos	9°19′S	47°50′W	10,840	10,545	−2.7
110	Manuel Alves Grande at Goiatins	7°43′S	47°20′W	9599	9636	0.4
111	Tocantins at Descarreto	5°46′S	47°29′W	296,357	298,559	0.7
112	Tocantins at Itaguatins	5°43′S	47°30′W	296,528	298,689	0.7
113	Claro at Montes Claros de Goiás	15°58′S	51°20′W	9547	9765	2.3
114	Vermelho at Travessão	15°32′S	50°42′W	5202	5242	0.8
115	Cristalino at Barra do Forquilinha (jusante)	12°54′S	50°51′W	8078	8039	−0.5
116	Mortes at Toriqueje	15°13′S	52°56′W	17,966	17,850	−0.6
117	Mortes at Xavantina	14°40′S	52°21′W	25,015	24,950	−0.3
118	Mortes at Trecho Médio	13°29′S	51°27′W	44,623	44,320	−0.7
119	Mortes at Santo Antônio do Leverger	12°04′S	50°51′W	57,680	55,346	−4.0
120	Araguaia at Torixoréu	16°15′S	52°30′W	19,049	19,100	0.3
121	Araguaia at Barra do Garças	15°50′S	52°12′W	36,537	36,432	−0.3
122	Araguaia at Bandeirantes	13°41′S	50°48′W	95,861	92,638	−3.4

the basin mask obtained in the previous step. After that, we digitized hundreds of smaller river sections in the Amazon and Tocantins basins from a 1:1,000,000 map of Northern South America, ensuring their proper geolocation. In an iterative procedure, part of the river network was modified to adjust the internal subbasin borders to match the drainage areas of 122 fluviometric stations, provided by ANEEL (Table 1). Some external borders were changed in this process too. After 17 iterations, we considered that the river network data set had acceptable quality, using the criteria that the drainage area determined using the river network data set would be within 5% of the drainage area reported by the ANEEL data set, for 122 stations spread throughout the basin (Table 1 and Figure 3). The only exception happened in station 32 (Aripuanã River at Prainha), with an error of −8.1%. In this case, we believe there is either an error in the ANEEL estimate of the drainage area or in the IBGE map we used, since it is impossible to reconcile the differences between them.

2.3. Refinement of the River Network to Assure Quality Sinuosity Data

[15] Finally, careful checking during the measurements of sinuosity ensures the accuracy of the river directions (see also section 4).

[16] Despite the careful procedure, there are some regions of the basin like the lower Negro River, where the river network data set is uncertain. Such regions are usually flat and flooded most of the year, making it difficult to define the direction of the river flow. Besides,

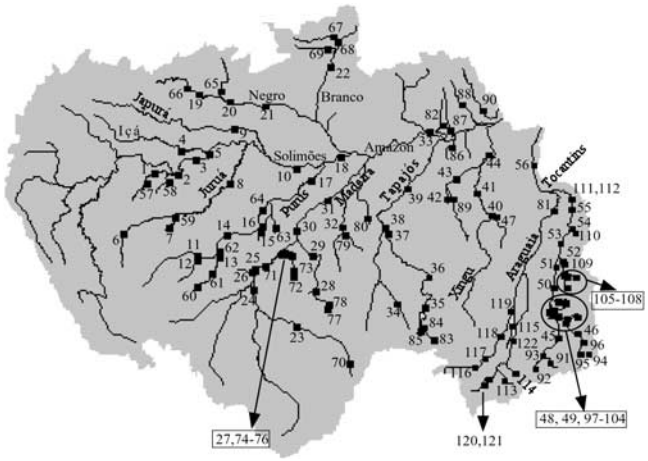

Figure 3. Location of fluviometric stations in the Amazon Basin. In this study, we utilize a network of 122 fluviometric stations provided by the ANEEL (Brazilian Agency for Waters and Electrical Energy).

those regions do not have ANEEL stations to be used as checkpoints.

3. River Discharge and River Stage

[17] Discharge data at specific checkpoints have been used to validate land-surface and atmospheric general circulation models. Most macrohydrological modeling studies so far in the Amazon Basin have used only a few stations to validate the discharge, with the exception of the study by *Costa and Foley* [1997], who used 56 stations, all of them with a drainage area greater than 30,000 km^2. Models now are using much finer resolution than previously, so we decided to expand the number of checkpoints to 122 stations, including stations with a much smaller drainage area. Considering that some current models simulate the height of water in the rivers, we also included data of river stage for model validation. The list of stations with discharge and stage data is provided in Table 1.

[18] The original daily river discharge and stage data set was obtained from ANEEL, the Brazilian National Agency for Waters and Electrical Energy. We present here a processed version of the original data, providing time series of monthly means only. Figure 4 shows a sample of time series of monthly mean river discharge for some stations.

4. Sinuosity

[19] In this section, we describe a data set of the sinuosity of the rivers of the Amazon and Tocantins basins. The sinuosity, sometimes called the meander ratio, is the ratio between the actual length of the river (measured on a map) and the length of the river as represented in the data set.

[20] The actual length of 111 sections of Amazonian rivers was measured on a 1:1,000,000 map of northern South America using a curvimeter (with three repetitions) and was then divided by the length of the same path in the data set. During the measurement, the river network data set was revised, so that the data set resembles the actual path of these river sections in the best possible way for a resolution of 5′.

[21] Assuming the fluvial geomorphologic processes were the same, the sinuosity measured for the main channel in the section is extrapolated to the tributaries in that subbasin. The sinuosity of the grid cells near the mouth of the Amazon River, downstream of the last measurements, was set to 1.00 (see also the methodology section of the river network data set).

[22] Sinuosity is a basin property that, when represented in a gridded framework, varies strongly according to the grid resolution. As the resolution increases, the actual path of the river tends to be represented more realistically by the river network data set, and the sinuosity tends to the value of 1.0. However, an analysis of Figure 5 shows that, even at the 5-min resolution, the sinuosity of the river can be as high as 2.3, in the area of the Purus and Juruá rivers. Rivers in those areas have meanders that are typically smaller than the dimensions of a grid cell (9 km).

[23] Several authors [*Vörösmarty et al.*, 1989; *Costa and Foley*, 1997; *Oki*, 1997; *Arora et al.*, 1999] have used sinuosity values between 1.1 and 1.8 for the Amazon Basin rivers, in grids with resolution varying between 0.5° and 2.0°. Our measurements actually show that, in parts of the Amazon Basin, even at a 5′ resolution, the meander ratio is much higher than the former estimates. Use of underestimated sinuosity parameters can introduce errors on the timing of the simulated river seasonal hydrograph and on the simulated amount of water stored in the river channel.

[24] In Figure 5, one can also notice that, in parts of the basin, the sinuosity assumes values that are smaller than the unity. Figure 6 shows schematically why this can happen. The cell-to-cell routing method assumes that the smallest river section is a straight line from the center of a grid cell to the center of the next grid cell. It is possible then that the actual river go through some grid cells without passing through their center.

5. Groundwater

[25] With a few exceptions, groundwater flow in macroscale hydrological models has been simulated in a very simple way, using, in most of the cases, a simple linear reservoir model. In these cases, the groundwater flow depends on an empirical constant, the residence time of the water in the groundwater pool. More advanced models, under development and testing, require the knowledge of the transmissivity of the surface aquifer. In addition, the depth of the water table has been used either in soil column models to parameterize the upward flow in the soil through capillarity or in integrated large-scale groundwater flow models, that include vertical and horizontal flow in the soil [*Abramopoulos et al.*, 1988; *Stieglitz et al.*, 1997].

[26] Measurements of the specific capacity of the aquifer and depth of the water table, collected at 81 wells spread throughout the Amazon Basin (Figure 7 and Table 2), were digitized from a 1:5,000,000 hydrogeological map of South America [*Brazil-DNPM/UNESCO*, 1996]. The measurements were interpolated using a Geographical Information System, producing maps of the depth of the water table (Figure 8) and of specific capacity (not shown). The specific capacity is then transformed into the aquifer transmissivity

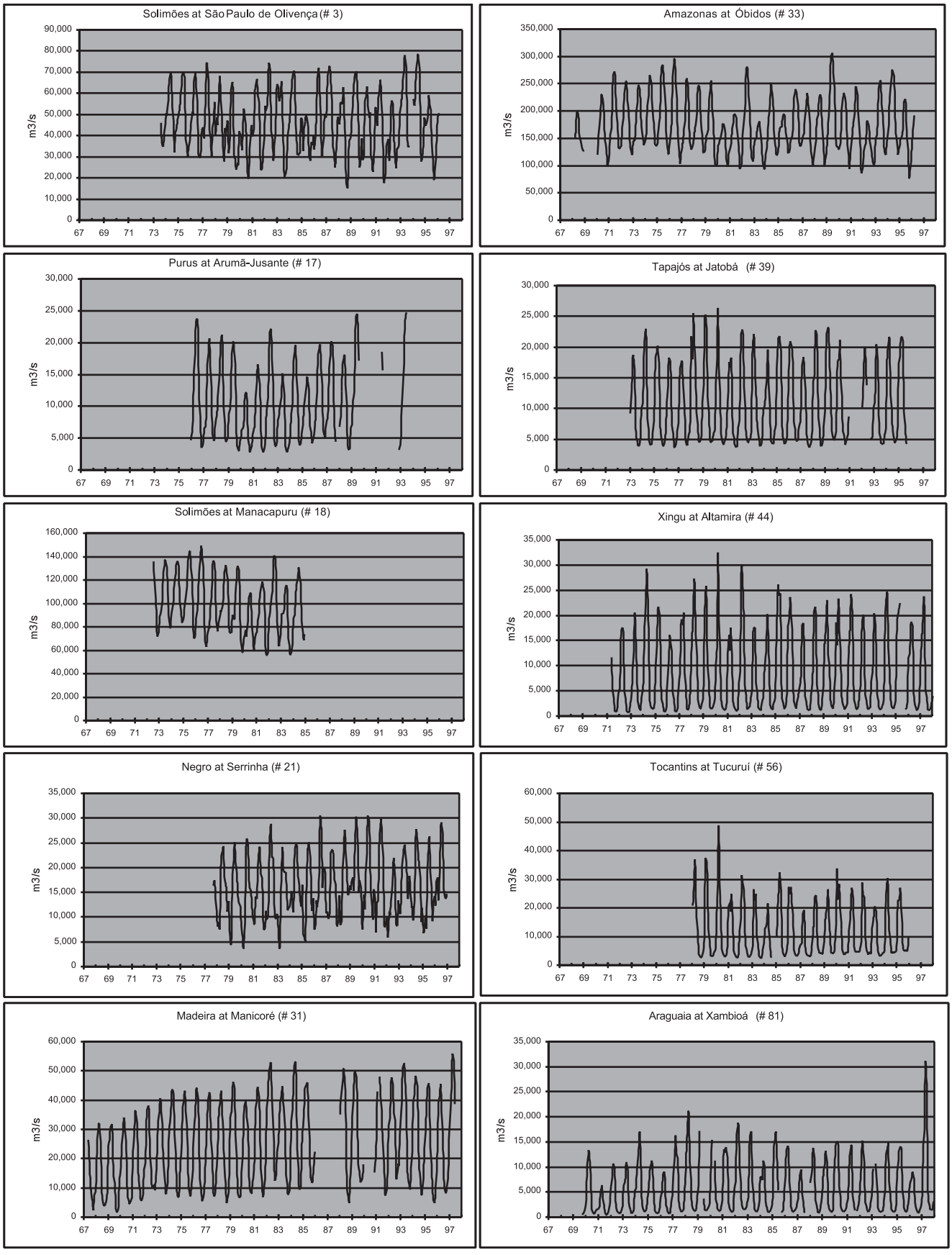

Figure 4. Sample of time series of river discharge.

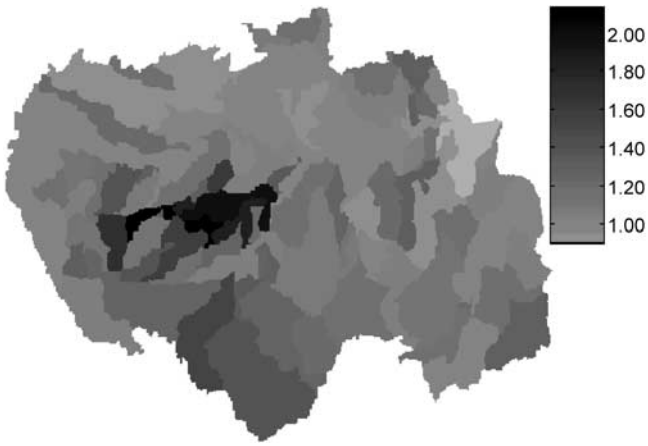

Figure 5. Sinuosity of the river sections in the Amazon Basin. It is assumed here that the geomorphologic processes within the same section are the same, and the sinuosity of the tributaries of that section is the same as the sinuosity of the main river in that section.

Figure 7. Location of wells. Groundwater data were collected in these 81 wells.

using the empirical relationship given by *Razack and Huntley* [1991] (equation (1))

$$T = 15.3\ S^{0.67} \quad (1)$$

where T is the aquifer transmissivity (m^2/day) and S is the specific capacity of the aquifer (m^2/day). Figure 9 shows the spatial distribution of the aquifer transmissivity.

[27] Obviously, the density of data collection points for the groundwater characteristics is too low. The spatial variability of the aquifer properties above must be much higher than what is shown in Figures 8 and 9. In addition, these are single measurements taken in a single day, which do not reflect seasonal and interannual variability of the depth of the water table. However, we consider this a first approximation of a data set required by a more physically based model of groundwater flow.

[28] In most of the basin, the water table is 5–15 m below the surface (Figure 8). In the upper parts of the basin, like in the Andes and in eastern border of the basin, the water table is usually deeper, sometimes reaching more than 30 m below the surface level. The water table is above the surface level in the southwest part of the basin, in a wetland area known as Llanos de Mojos, Bolivia.

[29] The aquifer transmissivity is a measure of the amount of water that can be transmitted horizontally through a unit width by a full-saturated thickness of the aquifer under a hydraulic gradient of 1 [*Fetter*, 1994, pp. 115]. For horizontal flow in an aquifer, it is usually a more useful parameter than the horizontal hydraulic conductivity. In the Amazon Basin, there is low correlation (ρ = 0.14) between the depth of the water table and the aquifer transmissivity. However, we find that the aquifers in the Andes and in the eastern border of the basin have higher transmissivity than in the rest of the basin.

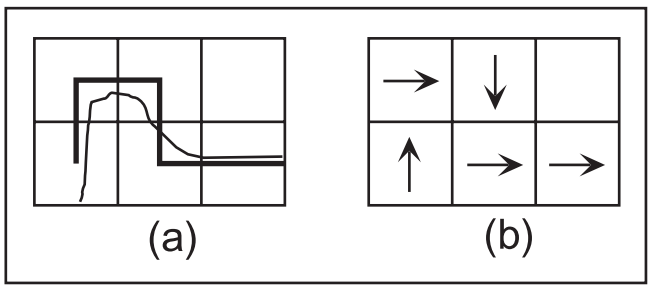

Figure 6. Diagram showing how sinuosity values smaller than one can happen. (a) Thin solid line is the actual path of the river and thick solid line is the river path as represented in the data set. (b) Equivalent river flow directions in the data set.

6. Summary and Conclusions

[30] A data set of river network, river sinuosity, and groundwater properties is presented for the Amazon and Tocantins basins, at the resolution of 5 min. Time series of river discharge and river stage, for 122 stations throughout the basin complete the data set. The data will be useful for implementing river routing schemes and further types of models that are based on river routing, such as sediment transport and river chemistry models. Applications of these models include macroscale hydrological studies and validation of climate models, in the context of the Amazon Basin.

[31] **Acknowledgments.** This research was supported by NASA through the LBA-Ecology and Surface Hydrology programs. Marcos H. Costa and T. R. Bustamante are CNPq fellows and F. A. Silva is a FAPEMIG fellow. The ANEEL daily river discharge and stage data was downloaded from http://hidroweb.aneel.gov.br.

[32] *Note:* The macrohydrological data set is available through anonymous ftp at ftp://ftp.ufv.br/dea/macrohydr and at http://www.sage.wisc.edu/datamodels.html.

References

Abramopoulos, F., C. Rosenzweig, and B. Choudhury, Improved ground hydrology calculations for Global Climate Models (GCMs): Soil water movement and evapotranspiration, *J. Clim.*, *1*, 921–941, 1988.

Arora, V. K., and G. J. Boer, A variable velocity flow routing algorithm for GCMs, *J. Geophys. Res.*, *104*, 30,965–30,979, 1999.

Table 2. Depth of the Water Table and Soil Parameters

Latitude	Longitude	Depth of the water table (m)	Specific capacity (m^3/h/m)	Aquifer transmissivity (m^2/day)
−4.10	−79.48	−6.10	7.00	473.9
−4.27	−70.02	−8.00	6.07	430.7
−4.97	−68.88	−15.00	0.87	117.2
−4.88	−66.83	−13.00	0.80	110.8
−5.72	−62.98	−15.00	1.96	202.0
−5.10	−60.27	−6.00	2.00	204.7
−5.30	−47.59	−6.00	10.50	621.8
−5.39	−46.69	−3.00	9.35	575.3
−6.45	−79.57	−3.70	19.00	925.1
−7.24	−78.19	–	11.60	664.7
−6.38	−64.33	−5.00	14.40	768.3
−7.22	−47.48	−3.00	40.00	1523.4
−8.89	−74.56	−9.20	–	–
−11.71	−46.86	−11.00	0.49	79.8
−11.25	−46.01	−80.00	1.53	171.1
−12.16	−75.22	−33.40	35.40	1403.7
−12.61	−69.08	0.00	2.00	204.7
−13.92	−66.70	−4.20	–	–
−15.96	−68.64	−9.75	6.60	455.5
2.00	−61.10	−5.00	0.59	90.3
0.18	−75.33	−3.50	3.70	309.1
−0.45	−78.48	5.00	2.70	250.3
−0.38	−76.92	−7.00	6.70	460.2
−1.48	−66.52	−4.00	1.89	197.1
−1.69	−65.38	−10.00	3.25	283.4
−0.88	−63.06	−9.00	4.64	359.7
−1.89	−60.67	−9.00	0.92	121.7
−1.89	−54.83	−3.50	8.70	548.2
−1.48	−50.49	−1.00	2.85	259.5
−2.89	−78.81	−2.30	0.30	57.4
−2.55	−66.00	−18.00	2.00	204.7
−3.54	−65.93	−18.00	2.00	204.7
−3.96	−61.32	−6.00	2.00	204.7
−2.94	−60.00	−6.00	2.00	204.7
−3.73	−59.17	−10.00	1.69	182.9
−2.99	−58.46	−8.00	4.88	372.1
−2.31	−54.72	9.00	3.30	286.3
−2.73	−52.18	−1.00	36.60	1435.4
−14.89	−64.74	−4.70	1.90	197.8
−14.83	−59.95	−4.00	3.80	314.7
−15.10	−56.39	−9.00	0.50	80.9
−16.00	−53.40	−13.00	0.56	87.2
−15.14	−48.04	−4.00	0.87	117.2
−16.32	−68.55	−0.95	4.50	352.4
−16.49	−68.69	−11.50	72.00	2258.6
−16.54	−68.36	8.11	7.12	479.3
−17.21	−68.00	−11.00	9.50	581.4
−17.14	−66.12	−11.30	0.90	119.9
−17.32	−66.51	1.00	5.40	398.2
−17.79	−67.15	2.39	4.40	347.2
−17.45	−65.76	1.00	11.21	649.6
−17.96	−64.18	−13.15	0.68	99.4
−18.00	−63.46	−29.50	0.22	46.7
−17.77	−63.11	1.00	2.50	237.7
−17.48	−63.20	−6.28	3.60	303.5
−17.50	−62.09	−17.65	0.60	91.4
−17.16	−63.68	−0.20	0.70	101.3
−17.17	−63.34	−3.50	0.40	69.6
−16.85	−63.27	1.00	74.00	2300.5
−16.72	−62.69	−8.00	1.13	139.6
−17.88	−60.25	−2.50	0.10	27.5
−16.76	−61.15	−11.00	0.43	73.1
−16.58	−60.83	−25.00	0.36	64.9
−16.41	−61.06	−22.00	0.30	57.4
−16.36	−58.49	−4.00	0.50	80.9
−17.52	−50.53	−32.00	0.48	78.7
−18.25	−67.14	−0.50	43.00	1599.0
−18.36	−67.22	−4.00	–	–
−18.43	−66.61	−8.80	0.45	75.4
−18.26	−64.00	−24.00	0.50	80.9
−19.78	−64.00	−20.00	1.80	190.8
−19.96	−63.67	−11.96	1.07	134.6
−19.44	−63.23	−2.90	0.20	43.8
−19.52	−63.74	−5.00	0.16	37.7
−19.29	−63.40	−34.50	2.50	237.7
−18.94	−62.98	−25.00	10.00	601.8
−18.76	−63.27	−4.88	1.04	132.1
−20.53	−63.54	−22.90	1.20	145.4
−20.56	−64.97	1.00	12.58	701.8
−21.12	−63.49	−21.85	5.40	398.2

Arora, V. K., F. H. S. Chiew, and R. B. Grayson, A river flow routing scheme for general circulation models, *J. Geophys. Res.*, *104*, 14,347–14,357, 1999.

Brazil-Departamento Nacional de Produção Mineral (DNPM)/United Nations Educational Scientific and Cultural Organization (UNESCO), Mapa hidrogeologico de America del Sur, 1996.

Brazil-Instituto Brasileiro de Geografia e Estatística (IBGE), International chart of the world on the millionth scale: Brazil, 46 pp., 1972.

Coe, M. T., Modeling terrestrial hydrologic systems at the continental scale: Testing the accuracy of an atmospheric GCM, *J. Clim.*, *13*, 686–704, 2000.

Costa, M. H., and J. A. Foley, Water balance of the Amazon Basin: Dependence on vegetation cover and canopy conductance, *J. Geophys. Res.*, *102*, 23,973–23,989, 1997.

Fetter, C. W., *Applied Hydrogeology*, 3rd ed., 691 pp., Prentice-Hall, Old Tappan, N. J., 1994.

Graham, S., J. S. Famiglietti, and D. R. Maidment, Five-minute, 1/2°, and 1° data sets of continental watersheds and river networks for use in regional and global hydrologic and climate system modeling studies, *Water Resour. Res.*, *35*, 583–587, 1999.

Hagemann, S., and L. Dümenil, A parameterization of lateral water flow for the global scale, *Clim. Dyn.*, *14*, 17–41, 1998.

Liston, G. E., Y. C. Sud, and E. F. Wood, Evaluating GCM land surface hydrology parameterizations by computing river discharges using a runoff routing models: Application to the Mississippi Basin, *J. Appl. Meteorol.*, *33*, 394–405, 1994.

Marengo, J. A., J. R. Miller, G. L. Russell, C. E. Rosenzweig, and F. Abramopoulos, Calculations of river-runoff in the GISS GCM: Impact of a new land-surface parameterization and runoff routing model on the hydrology of the Amazon River, *Clim. Dyn.*, *10*, 349–361, 1994.

Miller, J. R., and G. L. Russell, The impact of global warming on river runoff, *J. Geophys. Res.*, *97*, 2757–2764, 1992.

Miller, J. R., G. L. Russell, and G. Caliri, Continental scale river flow in climate models, *J. Clim.*, *7*, 914–928, 1994.

Oki, T., Validating the runoff from SLP-SVAT models using a global river routing network by one degree mesh, in *Proceedings of 13th Conference on Hydrology*, pp. 319–322, Am. Meteorol. Soc., Boston, Mass., 1997.

Razack, M., and D. Huntley, Assessing transmissivity from specific capacity data in a large and heterogeneous alluvial aquifer, *Ground Water*, *29*, 856–861, 1991.

Renssen, H., and J. M. Knoop, A global river routing network for use in hydrological modeling, *J. Hydrol.*, *230*, 230–243, 2000.

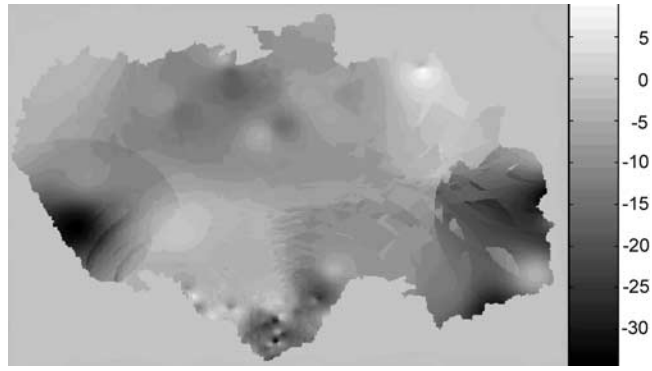

Figure 8. Depth of the water table (m). Negative values denote water below the surface level.

Figure 9. Aquifer transmissivity (m^2/day). The aquifer transmissivity is a measure of the amount of water that can be transmitted horizontally through a unit width by a full-saturated thickness of the aquifer under a hydraulic gradient of 1.

Sausen, R., S. Schubert, and L. Dümenil, A model of river runoff for use in coupled atmosphere-ocean models, *J. Hydrol.*, *155*, 337–352, 1994.

Stieglitz, M., D. Rind, J. Famiglietti, and C. Rosenzweig, An efficient approach to modeling the topographic control of surface hydrology for regional and global climate modeling, *J. Clim.*, *10*, 118–137, 1997.

Vörösmarty, C. J., B. Moore III, A. L. Grace, and M. P. Gildea, Continental scale models of water balance and fluvial transport: An application to South America, *Glob. Biogeochem. Cycles*, *3*, 241–265, 1989.

Vörösmarty, C. J., B. M. Fekete, M. Meybeck, and R. B. Lammers, Global system of rivers: Its role in organizing continental land mass and defining land-to-ocean linkages, *Glob. Biogeochem. Cycles*, *14*, 599–621, 2000.

R. G. Andrade, T. R. Bustamante, M. H. Costa, C. H. C. Oliveira, and F. A. Silva, Department of Agricultural Engineering, Federal University of Viçosa, Viçosa, Minas Gerais, Brazil. (mhcosta@mail.ufv.br)

M. T. Coe, Center for Sustainability and the Global Environment (SAGE), Institute for Environmental Studies, University of Wisconsin-Madison, Madison, WI, USA.